Analyst

Accepted Manuscript

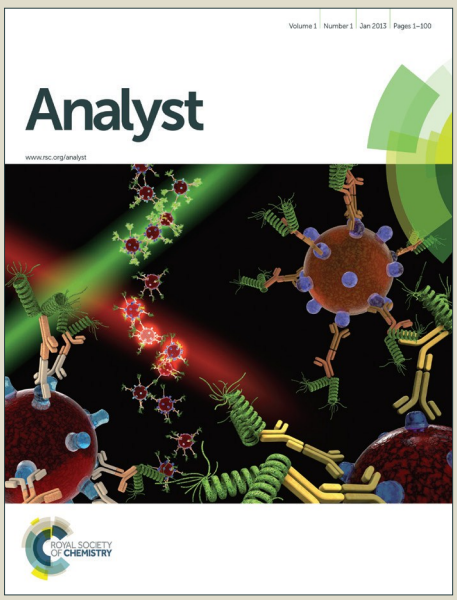

ROYAL SOCIETY OF CHEMISTRY

www.rsc.org/analyst

Development of a protease-resistant reporter to quantify BCR-ABL activity in intact cells.

Angela Proctor[#a], Imola G. Zigoneanu[#b], Qunzhao Wang[a], Christopher E. Sims[a], David S. Lawrence[ac] and Nancy L. Allbritton[*ab]

[#]Authors contributed equally to this work

[a]Department of Chemistry, University of North Carolina, Chapel Hill, NC, 27599, USA

[b]Joint Department of Biomedical Engineering, University of North Carolina, Chapel Hill, NC 27599, USA, and North Carolina State University, Raleigh, NC, 27695, USA

[c]Department of Chemical Biology and Medicinal Chemistry, School of Pharmacy, University of North Carolina, Chapel Hill, NC, 27599, USA

ABSTRACT

A peptidase-resistant ABL kinase substrate was developed by identifying protease-susceptible bonds on an ABL substrate peptide and replacing flanking amino acids with non-native amino acids. After an iterative design process, the lead, or designed, peptide X-A possesses a six-fold longer life in a cytosolic lysate than that of the starting peptide. The catalytic efficiency (k_{cat}/K_M) of purified ABL kinase for the lead peptide (125 s^{-1} μM^{-1}) is similar to that of the starting peptide (103 s^{-1} μM^{-1}) demonstrating preservation of the peptide's ability to serve as a kinase substrate. When incubated in cytosolic lysates, the lead peptide is slowly degraded into 4 fragments over time. In contrast, when loaded into intact cells, the peptide is metabolized into 5 fragments, with only 2 of the fragments corresponding to those in the lysate. Thus the two environments possess differing peptidase activities, which must be accounted for when designing peptidase-resistant peptides. In both settings, the substrate is phosphorylated by BCR-ABL

providing a readout of BCR-ABL activity. A small panel of tyrosine kinase inhibitors verified the substrate's specificity for BCR-ABL/ABL kinase activity in both lysates and cells in spite of the multitude of other kinases present. The designed peptide X-A acts as a long-lived BCR-ABL kinase reporter in the leukemic cells possessing the BCR-ABL mutation.

INTRODUCTION

Philadelphia chromosome positive (Ph+) cancer stem cells are a hallmark of chronic myelogenous leukemia (CML), with over 90% of CML patients expressing Ph+ cells.[1-6] The Ph chromosome results from a reciprocal translocation between the breakpoint cluster region (*bcr*) of chromosome 22 and the Abelson tyrosine kinase (*abl*) region of chromosome 9, forming a gene that encodes the fusion protein BCR-ABL. During the translocation event, the regulatory domain of ABL, normally located upstream of the kinase domain, is replaced by BCR, causing BCR-ABL to be constitutively active.[4,7,8] BCR-ABL hijacks the ABL pathway, resulting in, among other processes, increased proliferation and decreased apoptosis of cells possessing BCR-ABL.[4,8,9] The dependence of CML on BCR-ABL made it an ideal target for the first small molecule inhibitor specifically targeting a known oncogene.[10-13] Imatinib mesylate competes with ATP to bind in the catalytic domain of BCR-ABL to prevent the phosphorylation of BCR-ABL substrates.[10,14] As a front-line therapy, imatinib has been hugely successful, with an 8-year follow up of Phase III testing demonstrating 85% overall survival for imatinib-treated CML patients.[1,8] However, resistance to imatinib often develops, typically from acquired resistance that arises from one or more point mutations in the kinase domain.[8,9,15] Second and third generation inhibitors (*i.e.* dasatinib, ponatinib) have been developed to overcome these mutations, but are not usually considered until imatinib has failed.[8,9,16,17] Furthermore, there is a

small subset of CML patients who lack Ph+ cancer stem cells and do not benefit from therapies targeting these cells.[4,8] As therapy can be costly both financially and in terms of secondary health effects, it would be beneficial to measure both the biochemical activity of BCR-ABL and the sensitivity of patient cells to the inhibitor to direct optimal therapeutic choices and to monitor treatment.

Historically, BCR-ABL has been detected by the presence of the *bcr-abl* fusion gene using techniques such as chromosome banding and fluorescence in situ hybridization (FISH).[18-21] The cost, time, labor, and expertise required for these techniques and their limited sensitivity and specificity have driven the adoption of other methods for detection of *bcr-abl* in the clinical setting.[19] Genotyping technologies, such as traditional Sanger sequencing, microarray based screening, PCR-based techniques, and next-generation sequencing (NGS) are now supplanting these older approaches.[17,19,22-25] NGS has many benefits over the other genotyping technologies in detecting base substitutions, insertions, deletions, copy number alterations, and translocations and the cost per base pair is less than that of the more traditional techniques.[22] NGS can often detect lower copy numbers of *bcr-abl* mutants, providing an advantage in revealing the appearance of inhibitor-resistant mutations earlier than other techniques.[24] Protein detection techniques, such as mass spectrometry and flow cytometry, have been utilized to monitor BCR-ABL, but have not yet become mainstream clinical techniques.[26-29] The use of fluorescent antibodies against BCR-ABL, or its phosphorylated substrates (phospho-flow), have been employed in flow cytometry to characterize the presence of BCR-ABL on a cell-by-cell basis in both cell lines and patient samples.[28,29] A drawback in the above-mentioned techniques is that while detecting the presence of the fusion gene or its protein product, the methods do not quantitatively measure the biochemical activity of BCR-ABL. While phospho-flow can be used

to measure the presence of a phosphorylated BCR-ABL substrate, such as CRKL, even this technique is unable to detect constitutively or transiently active enzyme through quantification of substrate and product. A technique that quantifies the biochemical activity of BCR-ABL coupled with the capability to reliably analyze clinical samples, which typically contain a relatively small number of patient cells, would be of utility in assessing the likelihood of patient response to therapy.

Herein we describe the development of a rationally designed BCR-ABL peptide substrate that serves as a reporter for the direct quantification of BCR-ABL activity in cellular lysates and within intact cells.[30] Our design strategy utilizes non-native amino acids incorporated into the reporter at specific loci to impart stability to a peptide substrate that is otherwise rapidly degraded by intracellular proteases. Non-native amino acids are often used to expand the chemical properties available for proteins and peptides by selectively altering individual residues to feature properties not attainable with native amino acids.[31,32] Furthermore, non-native amino acids can serve as structural building blocks, conformational constraints, and protease-resistant residues in pharmacologically active agents, such as for enzymatic inhibitors and long-lived bioactive peptides.[33,34] It is this ability of non-native amino acids to stymie protease activity on peptides and proteins that led to their use in our generation of the peptidase-resistant BCR-ABL reporter described here.

Capillary electrophoresis separates analytes based on differences in electrophoretic mobilities, with analyte mass, shape, and charge all impacting this parameter.[35] The background electrolyte (BGE) utilized as the electrophoretic buffer can be finely tuned by adjusting the salt species, concentration, and pH or by addition of additives such as detergents or organics to influence net analyte charge or mobility. Proper BGE selection typically yields peaks with very

little band-broadening, translating to a high peak capacity and the ability to separate structurally-related analytes. In this work, the exquisite sensitivity and peak capacity of capillary electrophoresis coupled with laser-induced fluorescence detection (CE-LIF) permits the identification of proteolytic-susceptible peptide bonds due to the single-amino-acid resolution easily achieved by the CE-LIF technique. The optimized reporter serves as a robust BCR-ABL kinase reporter in both cellular lysates and within single cells with minimal degradation by intracellular proteases. Finally, cells pretreated with pharmacologic inhibitors were assayed for BCR-ABL activity to demonstrate the ability to analyze the relative effectiveness of individual inhibitors on BCR-ABL activity in living cells. Such data is aimed toward the idea of personalizing treatment options based on the unique biochemical phenotype of a specific patient's tumor.

MATERIALS AND METHODS

Materials. 5-carboxyfluorescein (5-FAM), 2-(6-chloro-1H-benzotriazole-1-yl)-1,1,3,3-tetramethylaminium hexafluorophosphate (HCTU), 9-fluorenylmethoxycarbonyl (Fmoc) amino acids, and the resins were purchased from ChemPep (Wellington, FL) and Novabiochem (San Diego, CA). N-Hydroxybenzotriazole (HOBt) was obtained from AnaSpec. Abl-1 human recombinant protein was obtained from Life Technologies (Carlsbad, CA). PTP1B inhibitor and bovine serum albumin (BSA) were purchased from Calbiochem (San Diego, CA). All other reagents for peptide synthesis and biochemical assays were ordered from Sigma-Aldrich (St. Louis, MO) or ThermoFisher Scientific (Waltham, MA). Cell culture reagents were procured as follows: Roswell Park Memorial Institute Media (RPMI-1640) from Cellgro (Manassas, VA), penicillin/streptomycin from Gibco (Grand Island, NY) and fetal bovine serum (FBS) from

Atlanta Biologicals (Flowery Branch, GA). The Baf/BCR-ABL murine cell line expressing BCR-ABL kinase was obtained from Dr. Brian Druker's lab at Oregon Health and Science University. Sodium orthovanadate and hydrogen peroxide were purchased from Sigma-Aldrich (St. Louis, MO). The kinase inhibitors dasatinib, masitinib, and sunitinib were obtained from LC Laboratories (Woburn, MA) and imatinib was purchased from Sigma (St. Louis, MO).

Peptide synthesis and purification. Full-length peptides and peptide fragment standards were synthesized by Fmoc solid phase peptide synthesis (Prelude peptide synthesizer, Protein Technologies, Tucson, AZ) as described previously[30] using a TentaGel Rink (TGR) resin for peptides amidated on the C-terminus and a 2-chlorotrityl chloride resin for peptide standards with a free carboxylic acid on the C-terminus. All peptides were labeled with 5-FAM at the N-terminus and purified via HPLC equipped with a 2489 UV/Visible detector (Waters 1512 Binary HPLC, Milford MA) and an Apollo 250 x 22 mm C18 column (5 μm particles; Grace, Columbia, MD) using a gradient of acetonitrile:water (3%-60%) with 0.1% trifluoroacetic acid. Peptide mass was confirmed by an Agilent 1200 series LC-MS with a 6110 Quadropole LC/MS detector (Agilent, Santa Clara, CA).

Cell Culture. Baf/BCR-ABL cells are a mouse B-cell lymphoma line that was stably transfected with and overexpresses BCR-ABL protein.[11] Baf/BCR-ABL cells were grown in RPMI-1640 media supplemented with 10% FBS, penicillin (100 units mL^{-1}), and streptomycin (100 mg mL^{-1}). The cells were kept in a humidified atmosphere of 37 °C with 5% CO_2 and were passaged into fresh media every 3-4 days.

Capillary electrophoresis. *In vitro* assay samples were analyzed by capillary electrophoresis coupled with laser-induced fluorescence detection (CE-LIF; 488 nm) using a ProteomeLab PA800 (Beckman Coulter, Fullerton, CA). Fused silica capillaries (Polymicro Technologies,

Phoenix, AZ) with an inner diameter of 50 μm, outer diameter of 360 μm, effective length of 20 cm, and a total length of 30 cm were pre-conditioned by rinsing sequentially with 1 M NaOH for 12 h, H_2O for 1h, 0.1 M HCl for 6 h, and H_2O for 12 h. Samples were diluted in the appropriate electrophoretic buffer to a final concentration of 50-250 nM prior to analysis. Capillaries were rinsed between each run with 1 M NaOH, H_2O, and buffer for 2 min by applying a pressure of 20 psi to the capillary inlet. Sample was hydrodynamically loaded into the capillary by applying 0.5 psi to the capillary inlet for 5 s and electrophoresis was initiated by applying a negative voltage to the outlet. For lysate samples, the voltage applied was 500 V cm^{-1} and for *in vitro* kinase assay samples, the voltage applied was 600 V cm^{-1}. The data was processed using commercial software (32 Karat, version 8.0, Beckman Coulter, Fullteron, CA) and represented graphically using Origin software (version 9.0, OriginLab Corporation, Northampton, MA).

The undiluted bulk lysate from cells pinocytically loaded with peptide was analyzed with a custom-built CE-LIF system as previously described in detail.[36] Capillaries were pretreated before use as described above and possessed a total length of 38 cm with an effective length of 20.5 cm and an inner diameter of 30 μm. The electrophoretic buffer was 100 mM tris, 100 mM tricine, pH 8.8 and a field strength of 210.5 V cm^{-1} was applied across the capillary for separations. Electrophoresis was initiated by applying a negative voltage to the capillary outlet while the inlet was held at ground. The data was analyzed and represented graphically using Origin 9.0 software.

Peptide degradation in a cellular lysate. The Baf/BCR-ABL cells were rinsed with and resuspended in phosphate buffered saline solution (PBS; 137 mM NaCl, 10 mM NaH_2PO_4, 27 mM KCl, 1.75 mM KH_2PO_4, pH 7.4), and then lysed using three freeze-thaw cycles. The supernatant was collected after centrifugation and total protein concentration was determined

using fluorescamine.[30] For assays, cytosolic lysate (3 mg mL^{-1} total protein) was incubated with 1 μM peptide substrate at 37 ºC. Aliquots were collected at different time points and the reaction inactivated with twice the aliquot volume of 200 mM HCl. A 0 min time point was prepared by inactivating the lysate with HCl prior to adding the peptide. Samples were diluted in the electrophoretic buffer (100 mM tris, 100 mM tricine, pH 8.1) to a final concentration of 50 nM peptide and analyzed by CE-LIF as described above. Migration times of proteolytic fragments were determined by sequentially adding each known fragment standard to the lysate samples and performing electrophoresis to identify unknown peaks. Triplicate measurements were performed using different cytosolic lysates.

***In vitro* phosphorylation by purified kinase.** Experiments were performed in triplicate by incubating a mixture of 29 μM fluorescently labeled peptide and 12 nM recombinant Abl-1 kinase in assay buffer (50 mM tris, 1 mM $MnCl_2$, 5 mM $MgCl_2$, 2 mM DTT, 1 mM ATP, pH 7.4) at 30 ºC. Aliquots were collected at varying time points and the enzyme was inactivated by heating the mixture at 95 ºC for 4 min. In addition, negative control samples without ATP were simultaneously collected. The aliquots were diluted in electrophoretic buffer (100 mM tris, 100 mM tricine, 5 mM SDS, pH 8.1) to a final peptide concentration of 60 nM and the amount of peptide reactant and product was quantified with CE-LIF. Peptide standards phosphorylated to completion were generated by incubating 29 μM substrate with 36 nM Abl-1 kinase in assay buffer at 30 ºC for 4 h. The mixture was inactivated by incubation at 95 ºC for 4 min and complete phosphorylation was confirmed by CE-LIF. Peaks on electropherograms were identified by co-mixing phosphorylated and non-phosphorylated peptide standards with samples.

Determination of kinetic parameters. The immobilized metal ion affinity-based fluorescent polarization (IMAP) assay (Molecular Devices, Sunnyvale, CA) was used to quantify the amount

of phosphorylated peptides following the manufacturer's instructions. Kinase assays were performed as described above with the following modifications: enzyme concentration was 6 nM and peptide concentration varied from 10 to 100 μM. For the IMAP assay, the samples were diluted to 100 nM with a buffer composed of 10 mM tris-HCl (pH 7.2), 10 mM $MgCl_2$, and 0.01% Tween-20. The amount of phosphorylated peptide was calculated based on a calibration curve obtained from measurements on co-mixtures of phosphorylated and non-phosphorylated peptide. A fluorescence plate reader (SpectrMax M5, Molecular Devices, Sunnvale, CA) with an excitation of 485 nm and emission of 525 nm was used.

Peptide phosphorylation in cellular lysates. Baf/BCR-ABL cells were rinsed twice with PBS and resuspended in the lysis buffer [Mammalian Protein Extraction Reagent (M-PER; Thermo Scientific, Waltham, MA) and 100 μM sodium pervanadate)]. No phosphorylation of peptide X-A was observed in the absence of the pan-phosphatase inhibitor, sodium pervanadate (data not shown) presumably due to the unrestrained activity of phosphatases under these conditions. Control experiments were performed using the same lysis buffer, but with 100 μM imatinib added. The mixture was agitated for 10 min, the supernatant collected by centrifugation, and total protein was determined by reaction with fluorescamine and comparison to standards of BSA. The reaction mixture comprising Baf/BCR-ABL cytosolic lysate (10 mg mL^{-1} total protein), reaction buffer (50 mM tris, pH 7.5, 1 mM $MnCl_2$, 5 mM $MgCl_2$, 2 mM DTT, 1 mM ATP) and peptide was incubated at 30 ^oC. Aliquots were collected at varying times and enzymes inactivated with an equal volume of 200 mM HCl. An initial 0 min time point was prepared by inactivating enzymes with HCl before adding the peptide. Samples were diluted in electrophoretic buffer (100 mM tris, 100 mM tricine, pH 8.1) to a final concentration of 250 nM

and analyzed by CE-LIF. Triplicate measurements were performed by using different cytosolic lysates.

Peptide phosphorylation in intact cells. Baf/BCR-ABL cells were loaded with peptide X-A using pinocytosis following the manufacturer's instructions (Influx, ThermoFisher Scientific, Waltham, MA.) 5 x 10^6 Baf/BCR-ABL cells were incubated for 1 h at 37 ºC in 1 mL of complete growth media supplemented with inhibitor or 1% DMSO as a control. Inhibitor concentrations were 50 µM imatinib, 15 nM dasatinib, 1 µM masitinib, or 300 nM sunitinib, with stock concentration diluted in DMSO such that the total DMSO amount in the media added to the cells was 1%.[37-40] The cells were loaded with peptide X-A by incubating for 10 min at 37 ºC in hypertonic loading solution containing 100 µM peptide X-A, 1 mM sodium pervanadate, and 50 µM PTP1B phosphatase inhibitor (25 µL per 5 x 10^6 cells.) Pinosomes were lysed in hypotonic RPMI-1640, releasing peptide X-A into the cytosol and initiating the biochemical reactions. Cells were transferred to complete growth media supplemented with tyrosine kinase inhibitor, 1 mM sodium pervanadate, and 50 µM PTP1B phosphatase inhibitor and allowed to recover for 10 min at 37 ºC. After recovery, cells were washed twice with PBS and the reactions terminated by heating at 95 ºC for 5 min. The total time that peptide X-A was in viable cells was 25 min. The cell lysate was clarified by pelleting at 14,000 x *g* for 15 min. The supernatant, containing the biochemical reaction products, was collected and stored at -20 ºC until immediately prior to CE analysis as described in the above "Capillary electrophoresis" section. Triplicate measurements were performed using different Baf/BCR-ABL cells.

RESULTS AND DISCUSSION

Optimization and characterization of an ABL kinase substrate. The ABL kinase substrate V-48B was previously rationally designed from an ABL substrate by sequential substitution of non-native amino acids to enhance resistance to protease degradation (Table 1).[30] While V-48B exhibits a 15-fold improved half-life in the face of cellular proteases relative to its parent sequence III-67B (Table 1), V-48B's degradation resistance is insufficient for kinase activity measurement when faced with the high concentration of peptidases within an intact cell. This is primarily due to hydrolysis of the peptide bond between the two alanine residues. We sought to enhance the protease resistance of V-48B while maintaining its ability to act as an ABL substrate by replacement of the labile bond's flanking residues. In past work by others, three non-native amino acids chemically similar to alanine [sarcosine, D-alanine, and (N-methyl)alanine] were demonstrated to impart peptide resistance to hydrolysis.[41-43] These residues impart resistance by either chemically modifying or reorienting the peptide backbone so that the peptidases no longer access or make appropriate contacts with the targeted peptide bond (Supplemental Figure S1).

Three peptides were synthesized with the amino-terminal alanine residue replaced by (N-methyl)alanine, sarcosine, or D-alanine (peptides VII-A, VII-B, and VII-C, Table 1). The peptides were incubated in a Baf/BCR-ABL cytosolic lysate and after varying times, aliquots were removed from the reaction mixture and assayed by CE. Over the course of 60 min, the parent peptides VII-A, VII-B, and VII-C were degraded into an additional 3, 3, and 4 peptides, respectively (Supplemental Figure S2). The percentage of intact peptide was plotted over time and the half-life ($t_{1/2}$) in the lysates calculated (Supplemental Figure S2, Table 1). The $t_{1/2}$ of the series VII peptides were similar to or poorer than that of peptide V-48B, indicating that the amino acid modifications do not prevent degradation by proteases. Indeed, sarcosine and (N-

methyl)alanine undesirably improves the peptide's suitability as a substrate for proteases relative to that of the starting peptide.

The ABL consensus sequence demonstrates a strong preference by the kinase for an alanine at the substitution site for the series VII peptides.[44] Whether this preference extended to alanine mimics (and potentially to non-native residues other than those assayed) was unclear. Before targeting this site for additional modifications, we sought to determine if the ABL kinase would tolerate substitutions at this site. Each peptide was incubated with purified ABL-1 kinase *in vitro* and phosphorylation was measured over time (Supplemental Figure S2). In all cases, none of the modified peptides demonstrated evidence of phosphorylation over the 120 min incubation, suggesting that even modifications with alanine-like residues at this location are intolerable to the kinase. Due to the lack of degradation resistance and poor substrate efficacy of the series VII peptides, substitutions at the alanine amino-terminal to the hydrolysis site were not pursued.

Characterization of peptides following replacement of the alanine carboxy-terminal to the hydrolysis site. In the second round of modifications, the alanine on the carboxy-terminal side of the susceptible bond was substituted with (N-methyl)alanine, sarcosine, or D-alanine (peptides VIII-A, VIII-B, and VIII-C, Table 1). These peptides were assessed for resistance to degradation by incubation in a Baf/BCR-ABL cytosolic lysate. After 60 min in the lysate, peptides VIII-A and VIII-C were metabolized into 5 peptide fragments and VIII-B into 4 fragments (Supplemental Figure S3). The (N-methyl)alanine (VIII-A) and sarcosine (VIII-B) substituted peptides were more stable than the parent peptides, with 22 ± 8% of intact VIII-A and 43 ± 10% of intact VIII-B remaining after 60 min (Figure 1A). The $t_{1/2}$ of peptides VIII-A and VIII-B are

1.3- and 2.5-fold longer, respectively, than that of the parent, V-48B (Table 1). The D-alanine-substituted peptide (VIII-C) did not exhibit an improved resistance to hydrolysis.

The consensus sequence for ABL substrates indicates a very slight preference for alanine at the substituted alanine in the series VIII peptides, suggesting that residues similar to alanine may be tolerated by the kinase at this location. The series VIII peptides were incubated with purified ABL-1 kinase (Figure 1B, Table 1) followed by measurement of phosphorylated peptide. Peptide VIII-C is minimally phosphorylated, indicating that a D-isomer in this position is not favored by the kinase, likely due to positioning of the side chain on the opposite side of the substrate. Peptides VIII-A and VIII-B were phosphorylated 6X and 1.5X faster than V-48B, respectively, suggesting that backbone modifications due to these two non-native amino acids do not alter the substrate's binding in the kinase's active site. Since VIII-B possesses the best protease resistance of the series VIII peptides while still remaining a good ABL substrate, VIII-B was further optimized.

Characterization of the peptide VIII-B fragments formed in a Baf/BCR-ABL cytosolic lysate. Although the sarcosine-containing peptide VIII-B displays a much longer lifetime in the cytosolic lysate than peptide V-48B, VIII-B was still degraded over time into four fragments. To determine which locations were susceptible to hydrolysis, all possible fluorescent peptide fragments were synthesized and characterized by electrophoresis. Under the electrophoretic conditions utilized, all of the fragment peptides were resolved from each other as well as from the intact parent peptide. Peptide VIII-B was incubated in a Baf/BCR-ABL lysate and each of the possible fluorescent peptide standards were sequentially added to the mixture to identify the unknown peaks in the electropherogram. The percentage of intact and fragmented peptide was then plotted as a function of time (Supplemental Figure S4). The 11-residue peptide is the first

initial fragment formed, appearing at a rate of 0.04 zmol pg^{-1} s^{-1}, nearly equal to that of the degradation rate of the intact peptide. This fragment is formed by removal of the alanine residue at the end of the peptide. Three other fragments, 2-, 5-, and 9-residue peptides, also formed, but in very low amounts relative to that of the 11-residue fragment. In the initial peptide V-48B, the most abundant fragment was the 5-residue peptide, which formed at a rate of 0.11 zmol pg^{-1} s^{-1}. In peptide VIII-B, this same 5-residue peptide fragment forms at a rate of 0.002 zmol pg^{-1} s^{-1}, approximately 55X slower, suggesting that conversion of the alanine to a sarcosine successfully blocks the proteases acting on the peptide bond between the two alanine residues.

Characterization of the 11-residue fragment of VIII-B as an ABL reporter. Peptide IX-A, identical to VIII-B but without the alanine residue at the C-terminus (Table 1), was assayed for resistance to proteolysis in a cell lysate. Unexpectedly, peptide IX-A degrades 1.5X faster than VIII-B with only 32 ± 3% of the peptide intact after 60 min (Figure 2.) In addition to the parent peptide, four peaks were observed on the electropherogram after 60 min and three of these peaks match the migration times of fragment peaks derived from peptide bond hydrolysis. However, the dominant fragment (43 ± 2% of all peptide) was not the result of peptide bond hydrolysis between two amino acids. Instead, this peptide is formed by conversion of the C-terminus carboxamide to the corresponding carboxylate, which was verified by comparison of the migration time of the synthesized standards. This result is surprising since deamidation was not observed for any of the prior peptides or for other kinase substrate peptides.[30,45] However, peptide deamidation does occur in biological peptides and proteins, though it is most often associated with the polar non-charged residues of asparagine and glutamine, and not lysine as observed here.[46,47] Deamidation typically depends on multiple attributes such as sequence and

3D structure, and is thought to be a post-translational modification that increases in incidence with organism age.[47]

The consensus sequence for ABL substrates is weighted toward those residues nearest to the phosphorylatable residue, with an isoleucine preferred at the -1 position, an alanine strongly preferred at the +1 position, and a proline preferred at the +3 position, relative to the phosphorylatable tyrosine.[44] No sequence preference is indicated at the +8 position suggesting that removal of the single terminal residue from peptide VIII-B to form IX-A might not diminish the ABL substrate properties of IX-A relative to that of VIII-B. When incubated with purified ABL-1 kinase, peptide IX-A demonstrated a $t_{50\%\,P}$ 2.8X better than that of peptide VIII-B (Figure 3, Table 1). The excellent ABL substrate properties of peptide IX-A and tolerance of the kinase for modifications at the C-terminus suggests that removal of the amidated terminus might yield an ABL reporter with increased protease resistance.

Characterization of the lead peptide X-A. Peptide X-A (identical to fragment xi from IX-A) was formed by removal of the amidated terminus of IX-A. Peptide X-A was incubated in a cytosolic lysate and its resistance to degradation in a cytosolic lysate quantified. The $t_{1/2}$ of X-A is 3.4X longer than that of peptide IX-A and nearly 6X longer than that of the starting peptide V-48B (Figure 3, Table 1). Peptide X-A was minimally degraded over the 60-min time span of the experiment with formation of small quantities of 4 fragments, the 5-, 4-, 2-, and 1-residue peptides (Figure 4). The 5-residue peptide (cleavage at the Ala-sarcosine bond) formed in the greatest quantity, representing 17 ± 0.6% of all peptide at 60 min, forming with an initial rate of 0.012 zmol pg^{-1} s^{-1}, 10X slower than it formed in the starting peptide V-48B. Thus this peptide bond continued to be protected by the sarcosine residue. Peptide X-A is the longest lived peptide in this small-scale library in spite of its free carboxylate terminus. Biologically, greater than 50%

of peptides are amidated *via* post-translational modifications in order to attain their maximum activity.[48,49] Synthetic peptides are often amidated to mimic this biological reality and to impart some protection of the peptide from exopeptidases.[50] However, in this case, removing the carboxamide moiety from peptide X-A actually improved its resistance to degradation. The positively-charged lysine residues at the C-terminus of peptides is often cleaved by carboxypeptidase B, a mammalian enzyme,[51] suggesting that this enzyme (and other similar enzymes) may not be highly active in these cells since the unprotected C-terminal lysine is relatively stable.

Peptide X-A was incubated with purified ABL-1 kinase *in vitro*, and aliquots were removed over time to quantify phosphorylation. Peptide X-A was phosphorylated 4X slower than precursor peptide IX-A and 2.4X slower than the starting peptide V-48B (Figure 3B). The free carboxylate of X-A adds a negatively charged terminus to the peptide. Abl kinase does not have a strong amino acid preference at this location (+7 relative to the tyrosine residue) on its native substrates and tolerates amino acids with negatively charged side chains in this position.[52] However, the +7 residue on a fully folded protein may be positioned so that no contact is made with the kinase, accounting for the tolerance of negatively charged residues at this position. In contrast, the +7 residue of an unstructured peptide is expected to be in proximity to the kinase surface for some fraction of time due to random molecular motions, and may be the cause of the decreased substrate phosphorylation.

To quantitatively compare the substrate suitability of the rationally designed peptide X-A to the starting peptide V-48B, their kinetic parameters were measured. Peptide X-A displays an improved K_M relative to that of peptide V-48B (15 ± 6 μM compared to 23 ± 6 μM), but suffers from a diminished turnover number (k_{cat} of 1,875 min^{-1} for peptide X-A compared to 2,375 min^{-1}

for peptide V-48B). However, the catalytic efficiency as evidenced by the k_{cat}/K_M is very similar for X-A (125 s^{-1} μM^{-1}) relative to that of V-48B (103 s^{-1} μM^{-1}). Furthermore, peptide X-A possesses a 6X improved resistance to degradation relative to V-48B, suggesting that X-A might act as a better reporter for Abl kinase in the presence of cytosolic proteases.

Peptide X-A as a reporter of BCR-ABL activity in cytosolic lysates. We next tested whether peptide X-A serves as a reporter of BCR-ABL activity in a cytosolic lysate while still resisting proteolytic degradation. Cell lysates are a cost-effective way to generate a reaction environment containing the native enzyme along with co-factors and regulatory elements found in the cell. Furthermore, both substrate and any inhibitors which are not cell-membrane permeant are readily assayed. Peptide X-A was incubated in a Baf/BCR-ABL lysate and aliquots removed over time and analyzed with CE-LIF to quantify peptide phosphorylation and degradation. X-A is readily phosphorylated in the lysate (Supplemental Figure S5B). When the lysate was incubated with the BCR-ABL kinase inhibitor imatinib prior to the addition of X-A, the degradation profile remained the same but phosphorylation was reduced to nearly zero, demonstrating that the phosphorylation of this peptide was accomplished by a kinase sensitive to imatinib, likely BCR-ABL. These results indicate that peptide X-A acts as a reporter of BCR-ABL activity in these cell lysates.

Peptide X-A as a reporter of BCR-ABL kinase activity within intact cells. We evaluated peptide X-A as a reporter of BCR-ABL activity in intact cells. Intact cell measurements offer distinct differences when compared to lysates in that the cell compartments and protein/organelle spatial relationships remain intact, providing an assay environment that is more biologically relevant than a lysate. Peptide X-A was easily introduced into intact cells using pinocytic loading and the cell with peptide incubated for 25 min prior to assay. Under these conditions, peptide X-

A was readily phosphorylated (23.5 ± 1.4%) in intact cells over the 25 min assay time. The peptide was also degraded in the intact cells into 5 different fragments (Figure 5), with the 5-mer fragment forming in the highest amounts, accounting for 21 ± 2% of all peptide. Of the 5 fragment peptides formed within the intact cells, only two (the 4-mer and 5-mer fragments) are the same as those formed in lysates, indicating that different peptidases are activated in the intact cells. The remaining three fragments that formed in the intact cells are the 7-, 9-, and 10-residue fragment peptides.

Small peptides are generally less specific for kinases than the full-length protein substrates due to their lack of the 3D structure and absence of accessory binding sites. To determine how well X-A behaves as a specific BCR-ABL substrate, the specificity of X-A for BCR-ABL was evaluated using a small panel of tyrosine kinase inhibitors. Imatinib and dasatinib inhibit BCR-ABL, c-KIT, and PDGFR at similar concentrations.[53] Masitinib was developed as a c-KIT inhibitor and only impacts BCR-ABL at micromolar concentrations.[39] Sunitinib is a potent inhibitor of VEGF and PDGF receptors and is not known to affect BCR-ABL at concentrations used to block VEGF and PDGF.[54] Inhibitors were used at 5X the IC_{50} concentrations for their target kinases[37-40] and inhibitor activity was verified by incubation with purified ABL-1 and measurement of X-A phosphorylation (Supplemental Figure S6). Cells were incubated with a tyrosine kinase inhibitor and then pinocytically loaded with X-A followed by measurement of X-A degradation and phosphorylation. The inhibitors did not impact degradation of X-A by cytosolic proteases (Figure 5A-B). Both imatinib and dasatinib significantly decrease the amount of X-A phosphorylation to 5.7 ± 0.3% and 3.7 ± 0.9%, respectively ($p < 0.001$ when compared to the DMSO vehicle). Masitinib also decreases phosphorylation of X-A relative to the control ($p < 0.05$). Suntinib does not significantly alter phosphorylation of X-A by the cell lysate.

Taken together these results suggest that under these conditions, the major kinase phosphorylating X-A is BCR-ABL. X-A acts as a long-lived BCR-ABL kinase reporter in these cells.

CONCLUSION

We have demonstrated the rational design of a BCR-ABL substrate reporter resistant to peptidase degradation that provides a direct readout of BCR-ABL activity in cellular lysates and intact cells. The bonds most susceptible to proteolysis were sequentially identified and flanking amino acids were replaced with non-native amino acids to yield increasingly stable substrates. The longer lifetime of the modified peptide enables the substrate to be loaded into intact cells followed by measurement of BCR-ABL activity within those cells. Utilization of a small panel of tyrosine kinase inhibitors strongly suggests that in these cells the reporter acts to report BCR-ABL activity as opposed to the activity of other kinases. A future goal of this project will be to optimize delivery into intact, single cells for assay of single-cell kinase activity, for example by generating a membrane-permeant version of the reporter

ACKNOWLEDGEMENTS

Funding for this work was provided by grants R01CA177993 and F32CA186748 from the National Institutes of Health.

REFERENCES

1. M. Breccia, G. Colafigli, M. Molica and G. Alimena, *Expert Opinion on Drug Safety*, 2016, **15**, 525-533.

2. A. de Klein, A. G. van Kessel, G. Grosveld, C. R. Bartram, A. Hagemeijer, D. Bootsma, N. K. Spurr, N. Heisterkamp, J. Groffen and J. R. Stephenson, *Nature*, 1982, **300**, 765-767.

3. G. A. Koretzky. *J Clin Invest*, 2007, **117**, 2030-2032.

4. J. M. Goldman, J. V. Melo, *N. Engl. J. Med.*, 2003, **349**, 1451-1464.

5. C. G. Geary. *Br. J. Haematol.*, 2000, **110**, 2-11.

6. N. Heisterkamp, J. R. Stephenson, J. Groffen, P. F. Hansen, A. de Klien, C. Bartram and G. Grosveld, *Nature*, 1983, **306**, 239-242.

7. M. W. N. Deininger, J. M. Goldman and J. V. Melo, *Blood*, 2000, **96**, 3343-3356.

8. C. Kujak, J. M. Kolesar, *Am J Health Syst Pharm*, 2016, **73**, 113-120.

9. E. Jabbour, H. Kantarjian, *Am. J. Hematol.*, 2016, **91**, 252-265.

10. B. J. Druker, S. Tamura, E. Buchdunger, S. Ohno, Segal, Gerald M. Fanning, Shane, J. Zimmermann and N. B. Lydon, *Nat. Med.*, 1996, **2**, 561-566.

11. F. X. Mahon, M. W. N. Deininger, B. Schultheis, J. Chabrol, J. Reiffers, J. M. Goldman and J. V. Melo, *Blood*, 2000, **96**, 1070-1079.

12. M. Okabe, Y. Uehara, T. Miyagishima, T. Itaya, M. Tanaka, Y. Kuni-Eda, M. Kurosawa and T. Miyazaki, *Blood*, 1992, **80**, 1330-1338.

13. M. Anafi, A. Gazit, A. Zehavi, Y. Ben-Neriah and A. Levitzki, *Blood*, 1993, **82**, 3524-3529.

14. E. Buchdunger, J. Zimmermann, H. Mett, T. Meyer, M. Müller, B. J. Druker and N. B. Lydon, *Cancer Res.*, 1996, **56**, 100-104.

15. A. Bansal, J. Radich, *Current Opinion in Hematology*, 2016, **23**, 115-120.

16. J. M. Goldman. *N. Engl. J. Med.*, 2012, **367**, 2148-2149.

17. M. W. Deininger, J. G. Hodgson, N. P. Shah, J. E. Cortes, D. Kim, F. E. Nicolini, M. Talpaz, M. Baccarani, M. C. Müller, J. Li, W. T. Parker, S. Lustgarten, T. Clackson, F. G. Haluska, F. Guilhot, H. M. Kantarjian, S. Soverini, A. Hochhaus, T. P. Hughes, V. M. Rivera and S. Branford, *Blood*, 2016, **127**, 703.

18. D. Y. Lee, H. I. Cho, Y. H. Kang, S. S. Yun, S. Y. Park, Y. S. Lee, Y. Kim and D. S. Lee, *Cancer Genet. Cytogenet.*, 2004, **152**, 1-7.

19. H. L. Lund, C. B. Hughesman, K. McNeil, S. Clemens, K. Hocken, R. Pettersson, A. Karsan, L. J. Foster and C. Haynes, *Anal Bioanal Chem*, 2016, **408**, 1079-1094.

20. K. Das, P. Tan, *Clin Genet*, 2013, **84**, 315-325.

21. D. Seong, H. M. Kantarjian, M. Albitar, R. Arlinghaus, J. Xu, M. Talpaz, M. B. Rios, J. Q. Guo, S. O'Brien and M. Siciliano, *Ann. Oncol.*, 1999, **10**, 955-959.

22. J. S. Ross, M. Cronin, *Am. J. Clin. Pathol.*, 2011, **136**, 527-539.

23. Z. Su, B. Ning, H. Fang, H. Hong, R. Perkins, W. Tong and L. Shi, *Expert Rev. Mol. Diagn.*, 2011, **11**, 333-343.

24. K. Machova Polakova, V. Kulvait, A. Benesova, J. Linhartova, H. Klamova, M. Jaruskova, C. de Benedittis, T. Haferlach, M. Baccarani, G. Martinelli, T. Stopka, T. Ernst, A. Hochhaus, A. Kohlmann and S. Soverini, *J. Cancer Res. Clin. Oncol.*, 2015, **141**, 887-899.

25. J. Linhartova, L. Hovorkova, S. Soverini, A. Benesova, M. Jaruskova, H. Klamova, J. Zuna and K. Machova Polakova, *Mol Cancer*, 2015, **14**.

26. S. B. Breitkopf, M. Yuan, G. A. Pihan and J. M. Asara, *Proc Natl Acad Sci U S A*, 2012, **109**, 16190-16195.

27. Wendy T. Parker, Rebecca M. Lawrence, Musei Ho, Darryl L. Irwin, Hamish S. Scott, Timothy P. Hughes and Susan Branford, *Journal of Clinical Oncology*, 2011, **29**, 4250.

28. A. Hamilton, L. Elrick, S. Myssina, M. Copland, H. Jørgenson, J. V. Melo and T. Holyoake, *Leukemia*, 2006, **20**, 1035-1039.

29. F. Weerkamp, E. Dekking, Y. Y. Ng, van der Velden, V H J, H. Wai, S. Boettcher, M. Brueggemann, van der Sluijs, A J, A. Koning, N. Boeckx, N. Van Poecke, P. Lucio, A. Mendonca, L. Sedek, T. Szczepanski, T. Kalina, M. Kovac, P. G. Hoogeveen, J. Flores-Montero, A. Orfao, E. Macintyre, L. Lhermitte, R. Chen, Brouwer-De Cock, K A J, A. van der Linden, A. L. Noordijk, W. M. Comans-Bitter, F. J. T. Staal and van Dongen, J J M, *Leukemia*, 2009, **23**, 1106-1117.

30. A. Proctor, Q. Wang, D. S. Lawrence and N. L. Allbritton, *Analyst*, 2012, **137**, 3028-3038.

31. R. B. Quast, D. Mrusek, C. Hoffmeister, A. Sonnabend and S. Kubick, *FEBS Letters*, 2015, **589**, 1703-1712.

32. A. Stevenazzi, M. Marchini, G. Sandrone, B. Vergani and M. Lattanzio, *Bioorganic & Medicinal Chemistry Letters*, 2014, **24**, 5349-5356.

33. C. J. Vickers, G. E. González-Páez, K. M. Litwin, J. C. Umotoy, E. A. Coutsias and D. W. Wolan, *ACS Chem. Biol.*, 2014, **9**, 2194-2198.

34. N. Yin, M. A. Brimble and Wen, Paul WR Harris and Jingyuan, *Medicinal Chemistry*, 2014, **2014**.

35. R. Weinberger, in *Practical Capillary Electrophoresis*, Academic Press, London, 1st ed, 1993.

36. A. Proctor, S. G. Herrera-Loeza, Q. Wang, D. S. Lawerence, J. J. Yeh and N. L. Allbritton, *Anal. Chem.*, 2014, **86**, 4573-4580.

37. C. Ly, A. F. Arechiga, J. V. Melo, C. M. Walsh and S. T. Ong, *Cancer Res*, 2003, **63**, 5716-5722.

38. L. J. Lombardo, F. Y. Lee, P. Chen, D. Norris, J. C. Barrish, K. Behnia, S. Castaneda, L. A. M. Cornelius, J. Das, A. M. Doweyko, C. Fairchild, J. T. Hunt, I. Inigo, K. Johnston, A. Kamath, D. Kan, H. Klei, P. Marathe, S. Pang, R. Peterson, S. Pitt, G. L. Schieven, R. J. Schmidt, J. Tokarski, M. Wen, J. Wityak and R. M. Borzilleri, *J. Med. Chem.*, 2004, **47**, 6658-6661.

39. P. Dubreuil, S. Letard, M. Ciufolini, L. Gros, M. Humbert, N. Castéran, L. Borge, B. Hajem, A. Lermet, W. Sippl, E. Voisset, M. Arock, C. Auclair, P. S. Leventhal, C. D. Mansfield, A. Moussy and O. Hermine, *PLOS ONE*, 2009, **4**, e7258.

40. J. Guo, P. A. Marcotte, J. O. McCall, Y. Dai, L. J. Pease, M. R. Michaelides, S. K. Davidsen and K. B. Glaser, *Mol Cancer Ther*, 2006, **5**, 1007-1013.

41. T. T. Tran, H. Treutlein and A. W. Burgess, *Protein Eng., Des. Sel.*, 2006, **19**, 401-408.

42. R. Tugyi, K. Uray, D. Iván, E. Fellinger, A. Perkins and F. Hudecz, *PNAS*, 2005, **102**, 413-418.

43. L. Gentilucci, R. De Marco and L. Cerisoli, *Curr. Pharm. Des.*, 2010, **16**, 3185-3203.

44. Z. Songyang, K. L. Carraway III, M. J. Eck, S. C. Harrison, R. A. Feldman, M. Mohammadi, J. Schlessinger, S. R. Hubbard, D. P. Smith, C. Eng, M. J. Lorenzo, B. A. J. Ponder, B. J. Mayer and L. C. Cantley, *Nature*, 1995, **373**, 536-539.

45. A. Proctor, Q. Wang, D. S. Lawrence and N. L. Allbritton, *Anal. Chem.*, 2012, **84**, 7195-7202.

46. D. Gervais. *J. Chem. Technol. Biotechnol.*, 2016, **91**, 569-575.

47. N. E. Robinson, A. B. Robinson, *PNAS*, 2001, **98**, 12409-12413.

48. D. J. Merkler. *Enzyme and Microbial Technology*, 1994, **16**, 450-456.

49. K. Kim, B. L. Seong, *Biotechnol. Bioprocess Eng.*, 2001, **6**, 244-251.

50. B. M. Dunn, in*Peptide Chemistry and Drug Design*, John Wiley & Sons, 2015.

51. J. E. Folk, K. A. Piez, W. R. Carroll and J. A. Gladner, *J. Biol. Chem.*, 1960, **235**, 2272-2277.

52. J. Colicelli. *Sci Signal*, 2010, **3**, re6.

53. E. Weisberg, P. W. Manley, S. W. Cowan-Jacob, A. Hochhaus and J. D. Griffin, *Nat. Rev. Cancer*, 2007, **7**, 345-356.

54. D. B. Mendel, A. D. Laird, X. Xin, S. G. Louie, J. G. Christensen, G. Li, R. E. Schreck, T. J. Abrams, T. J. Ngai, L. B. Lee, L. J. Murray, J. Carver, E. Chan, K. G. Moss, J. Ö Haznedar, J. Sukbuntherng, R. A. Blake, L. Sun, C. Tang, T. Miller, S. Shirazian, G. McMahon and J. Cherrington, *Clin. Cancer Res.*, 2003, **9**, 327-337.

FIGURES

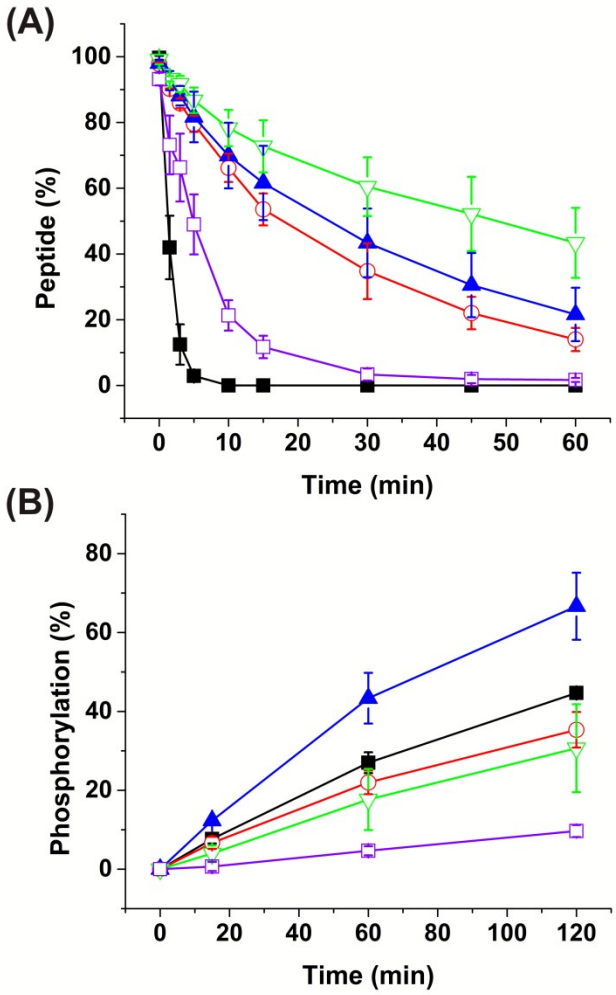

Figure 1: Properties of the series VIII peptides. (A) Degradation in a Baf/BCR-ABL cellular lysate. (B) *In vitro* phosphorylation with purified Abl-1 kinase. The symbols are defined as: black filled square (peptide III-67B), red open circle (peptide V-48B), blue closed triangle (peptide VIII-A), green open triangle (peptide VIII-B), and purple open square (peptide VIII-C).

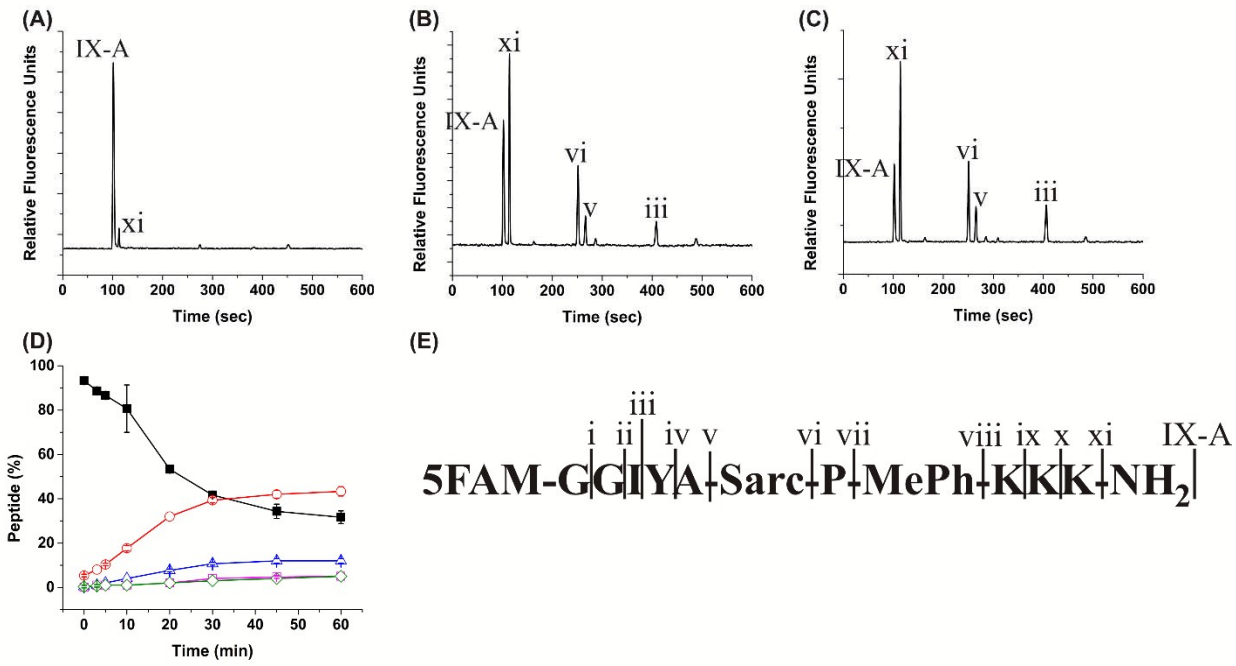

Figure 2: Electropherograms of peptide IX-A incubated in a Baf/BCR-ABL cytosolic lysate for 0 (A), 30 (B), or 60 (C) min. The electrophoretic buffer utilized was 100 mM tris, 100 mM tricine, pH 8.1. Degradation of IX-A and formation of peptide fragments over time (D). The symbols are defined as follows: black closed square (peptide xii), red open circle (peptide xi), blue open triangle (peptide vi), pink open square (peptide v), green open diamond (peptide iii). (E) The uppercase letters are the single amino acid abbreviations for peptide IX-A's sequence, with Sarc the abbreviation for sarcosine, and MePh the abbreviation for *N*-methyl phenylalanine. The roman numerals indicate the cleavage locations that generated the indicated peptide fragment.

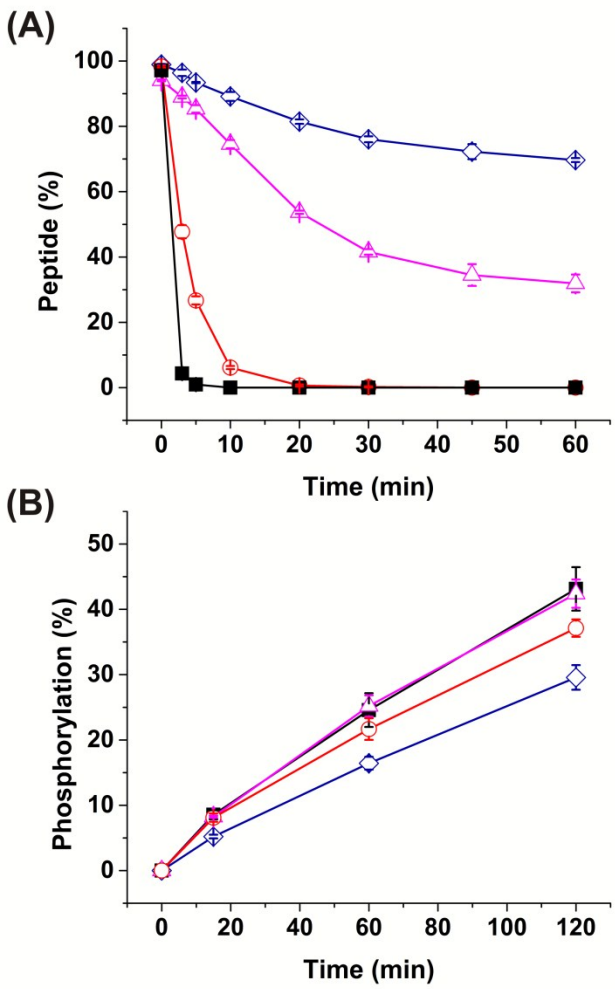

Figure 3: Properties of the IX-A and X-A peptides. (A) Percentage of intact peptide in a Baf/BCR-ABL cellular lysate. (B) *In vitro* phosphorylation of the peptides with purified Abl-1 kinase. The symbols are defined as: black filled square (peptide III-67B), red open circle (peptide V-48B), pink open triangle (peptide IX-A), and blue open diamond (peptide X-A).

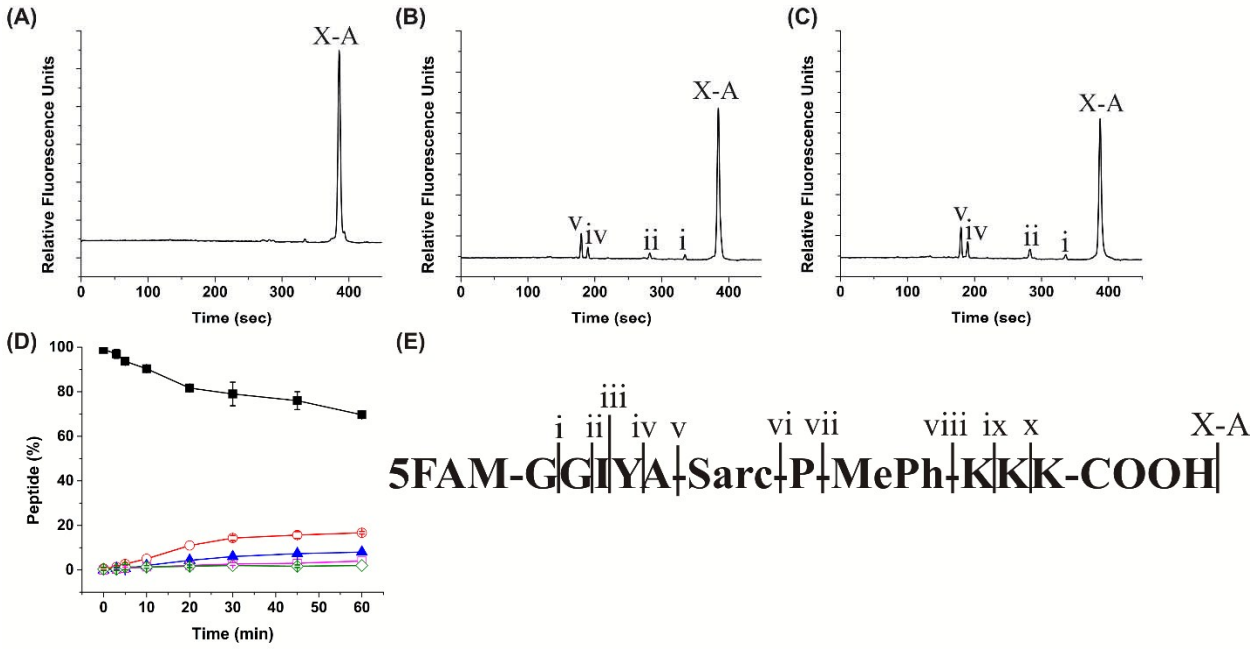

Figure 4: Electropherograms of peptide X-A incubated in a Baf/BCR-ABL cytosolic lysate for 0 (A), 30 (B), or 60 (C) min. The electrophoretic buffer utilized was 100 mM tris, 100 mM tricine, 5 mM SDS, pH 8.1. (D) The percentage of X-A present as intact X-A and peptide fragments is shown over time. The symbols are defined as follows: black closed square (peptide xi), red open circle (peptide v), blue closed triangle (peptide iv), pink open square (peptide ii), green open diamond (peptide i). (E) The uppercase letters are the single amino acid abbreviations for peptide X-A's sequence, with Sarc the abbreviation for sarcosine, and MePh the abbreviation for *N*-methyl phenylalanine. The roman numerals indicate the cleavage locations that generate the indicated peptide fragment.

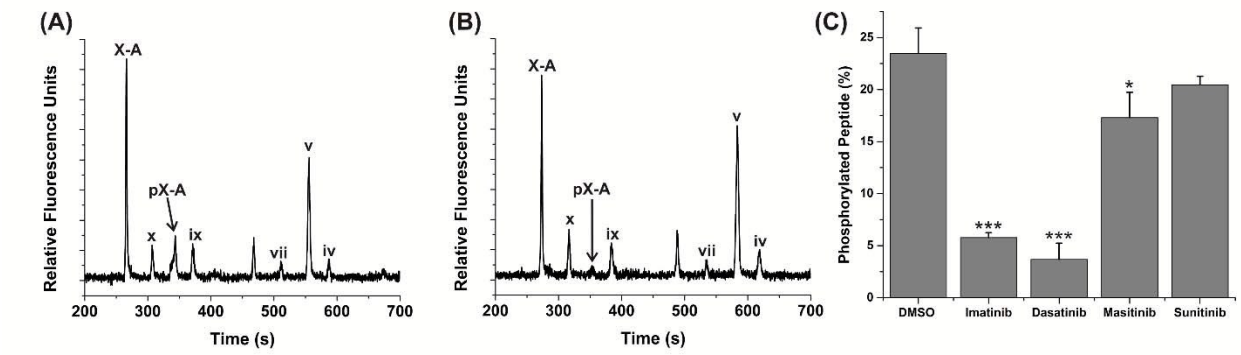

Figure 5: Select electropherograms from pinocytically loaded cells treated with DMSO vehicle (A) or dasatinib (B) prior to loading. Phosphorylated X-A (pX-A) is indicated by the arrow and the roman numerals are the fragments identified for peptide X-A in Figure 4. The electrophoretic buffer utilized was 100 mM tris and 100 mM tricine, pH 8.8. (C) Phosphorylation of peptide X-A in Baf/BCR-ABL cells pre-treated with or without tyrosine kinase inhibitors. *** P-value ≤ 0.001 and * P-value ≤ 0.05 when compared to the DMSO control.

TABLES

Table 1: Properties of the peptides tested.

Peptide Name	Sequence	$t_{1/2}$[a] (min)	$t_{50\%\ P}$[b] (min)
III-67B*	5FAM-GGA**Y**AAPFKKKA	1.3	190
V-48B*	5FAM-GGI**Y**AAP-MePhe-KKKA	19.4	400
VII-A	5FAM-GGI**Y**-MeAla-AP-MePhe-KKKA	1.6	NP
VII-B	5FAM-GGI**Y**-Sarc-AP-MePhe-KKKA	5.5	NP
VII-C	5FAM-GGI**Y**-DAla-AP-MePhe-KKKA	17.9	NP
VIII-A	5FAM-GGI**Y**A-MeAla-P-MePhe-KKKA	25.8	68
VIII-B	5FAM-GGI**Y**A-Sarc-P-MePhe-KKKA	48.7	650
VIII-C	5FAM-GGI**Y**A-DAla-P-MePhe-KKKA	5.1	>100,000
IX-A	5FAM-GGI**Y**A-Sarc-P-MePhe-KKK	32.1	232
X-A	5FAM-GGI**Y**A-Sarc-P-MePhe-KKK-COOH	110	945

*Data from previous work.[30] [a] $t_{1/2}$ is the time at which 50% of the peptide was degraded in the cytosolic lysate (3 mg mL^{-1} total protein). [b] $t_{50\%\ P}$ is the time required for 50% of the peptide to be phosphorylated by Abl-1 kinase under the conditions employed using 12 nM of kinase. NP indicates no phosphorylation occurred. Peptides are amidated on the C-terminus unless noted otherwise. Abbreviations are the standard single letter amino acids, except for the following: MePhe (*N*-methylated phenylalanine), MeAla (*N*-methylated alanine), Sarc (sarcosine), DAla (D-alanine).